Evaluation of Signal-to-Noise and Distortion Ratio Degradation in Nonlinear Systems

Pedro Miguel Lavrador, *Student Member, IEEE*, Nuno Borges de Carvalho, *Member, IEEE*, and José Carlos Pedro, *Senior Member, IEEE*

***Abstract*—This paper presents a new figure-of-merit to evaluate signal-to-noise and distortion (SINAD) ratio degradation in nonlinear systems, herein referred to as the noise and distortion figure (NDF). In order to obtain a mathematical formula for this NDF, the best linear approximation calculation is presented for memoryless and dynamic nonlinear systems, which can be modeled by a finite Volterra series. To the best of the authors' knowledge, this is the first time such an attempt of calculating the NDF for a nonlinear and dynamic system is made. NDF results are discussed in both types of systems by means of numerical simulations of systems up to the third order.**

***Index Terms*—Correlation, nonlinear distortion, spectral analysis, Volterra series.**

I. Introduction

SIGNAL-TO-NOISE ratio (SNR) in real communication systems can be severely degraded when signals are processed by nonlinear components. That degradation is normally attributed to two different impairments: linear additive noise and nonlinear distortion [1].

In order to account for the additive noise, the figure-of-merit noise figure (NF) is normally used, while the third-order intercept point IP_3 can be made to play a correspondent role for nonlinear distortion degradation.

Unfortunately, until now, the complex behavior of nonlinear distortion has prevented the integration of these two SNR degradation figures, forcing the design engineer to evaluate any link budget in two different steps: looking for the small amplitude signal limitations determined by additive noise, and its high-level end imposed by nonlinear distortion. Only by taking into account those two perturbation causes can the design engineer maximize the communication systems' dynamic range.

In an effort to understand the relation between these two signal perturbation figures-of-merit, in [2], Geens and Rolain have detected some problems when measuring the NF in the presence of nonlinearities and proposed a new NF to circumvent those problems. Nevertheless, and due to the excitation signals that were used, the results obtained with this new formulation of the NF can be disastrous, as it predicts certain zones of improvement in the output SNR (SNR_o), an obviously impossible outcome in practical situations.

Furthermore, this study restricted its analysis to memoryless nonlinear systems, which constitutes a severe limitation if applied to modern wide-band wireless components that are known to exhibit strong nonlinear memory effects [3], [4].

One of the first and most important difficulties imposed by nonlinear distortion analysis is its dependence on the type of excitation signal. That issue, for a long time recognized in the nonlinear systems' identification field [5], [6], demands a careful selection of a convenient signal class.

Although RF and microwave engineers tend to represent their telecommunication signals by a pure sinusoid, it is already known that such a class of signals is totally inadequate. In fact, it lacks nonnull bandwidth, an amplitude envelope, and the random behavior typical of real information signals. Although the two-tone has also been widely adopted for nonlinear distortion testing, it still suffers from the fact that it only involves a sinusoidal envelope of deterministic behavior, two properties especially relevant in wide-band nonlinear dynamic systems. A much better signal class used to represent real communication signals that does not suffer from any of these drawbacks is the band-limited white Gaussian noise, which will, therefore, be adopted for the present definition of a new figure-of-merit intended to be a metric of SNR degradation in the presence of additive noise and nonlinear distortion.

The second issue worthy of discussion is the separation of the system's output into its signal and distortion components. A useful criterion should be to use the same separation undertaken in modern wireless receivers, as it would immediately lead to practically significant transmission quality figures as bit error rate. Thus, in that sense, we will take as a signal everything that contains information eventually processed by a linear dynamic operator, and as distortion, any remaining part. This way, it is possible to classify as a signal the outcome of the so-called best linear approximation (BLA) [6], which governs the linear behavior of the output signal versus the input excitation, and then use cross-correlation to uniquely identify it. The dependence of the system's BLA (gain in a memoryless system) on the input has already been discussed in the 1960s [7].

With those two assumptions in mind, it was then possible to correctly divide the output useful signal from the noise distortion, and then quantify the signal to noise and distortion ratio (SINAD) at the output (SINAD_0) .

In this paper, the approach followed in [2] is first discussed and its drawbacks explained. By using white Gaussian noise as the standard excitation, and cross-correlation techniques, it is

Manuscript received April 17, 2003; revised September 18, 2003. This work was supported by the Portuguese Science Bureau Fundação para a Ciência e a Tecnologia (F.C.T.) under Project POCTI/ESE/37531/2002–OPAMS. The work of P. M. Lavrador was supported in part by the F.C.T. under Ph.D. Grant 6835/2001. The work of J. C. Pedro was supported in part by the F.C.T. under Sabbatical Grant SFRH/BSAB/315/2002.

The authors are with the Telecommunications Institute, University of Aveiro, 3810-193 Aveiro, Portugal.

Digital Object Identifier 10.1109/TMTT.2004.823543

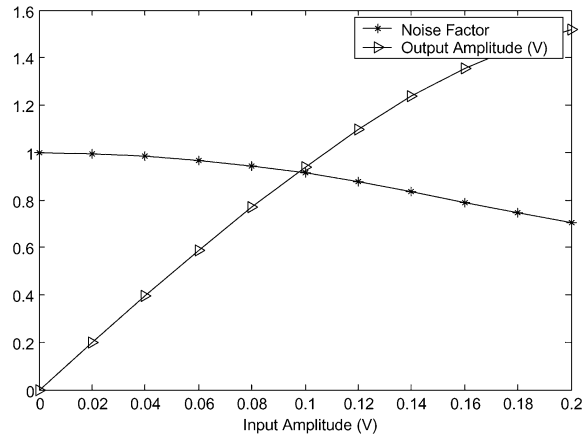

Fig. 1. NF proposed in [2]. Variation with the input power for a system with parameters $G = 100$ and $\alpha = 60$, as indicated in this paper.

then shown how the BLA can be determined for general memoryless and dynamic nonlinear Volterra systems; this way allowing the identification of the desired signal and noise components involved in the system's output.

A new noise and distortion figure (NDF) relating the input and output SINADs, SINAD_i and SINAD_o is then proposed.

In order to validate the derived closed-form expressions for the newly defined NDF, a time-domain simulation was performed for a typical dynamic nonlinear system, of third order, and the results compared with the proposed theoretical values.

II. Nonlinear NF Revisited

An important figure used to measure the degradation of signal quality between input and output is the NF, which relates the signal to noise ratio at the input (SNR_i) to the signal to noise ratio at the output (SNR_0). Geens and Rolain [2] have proven that the presence of nonlinear distortion influences the measured NF value, and proposed a new setup for measuring the NF using a single tone as a test signal.

Using this approach, they reached the following expression for the NF:

$$\mathrm{NF} = \frac{\mathrm{SNR}_{\mathrm{in}}}{\mathrm{SNR}_{\mathrm{out}}} = \frac{G + \frac{27}{8}\alpha^2 A^4 - 3\alpha\sqrt{G}A^2}{G + \frac{9}{16}\alpha^2 A^4 - \frac{3}{2}\alpha\sqrt{G}A^2} \tag{1}$$

where G is the linear power gain, α is a third-order voltage gain, and A the input tone amplitude. A closer look into (1) reveals that there are certain zones of input signal voltage in which the NF can be smaller than one, as shown in Fig. 1.

This result is strange since it indicates that the system can, in fact, improve SNR from the input to the output, in a certain sense, eliminating input noise.

A closer look into this theoretical result shows that the apparent gain in the SNR is caused by the different compression imposed to each signal: a sinusoid and white Gaussian noise. Actually, it is known [8] that when two different signals excite a nonlinear system, in which one is of much larger amplitude than the other, the compression of the smaller one is mainly determined by the level of the strong signal. In this case, the sinusoidal signal is the dominant component, therefore, determining a greater compression to the noise. In fact, the relation between the output sinusoid and noise will be improved due to the extra compression imposed to noise level.

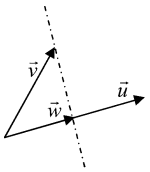

Fig. 2. Geometric representation of the method used to determine the output signal component.

The referred problems associated to this approach can be traced to the use of a single sinusoid as the input signal. Actually, there is no input noise perturbing the signal since the signal has a null spectral bandwidth and, thus, there is no noise power inside the signal bandwidth. Additionally, since this test signal has a constant envelope, it is also unable to generate uncorrelated nonlinear distortion, also know as nonlinear distortion noise [6].

A more appropriate alternative would be the use of a test signal similar to a real communications signal, e.g., Gaussian noise, since it has nonzero bandwidth, allowing the inclusion of effective additive noise and uncorrelated nonlinear distortion effects. Beyond that, it has statistical properties similar to the ones of real signals.

III. Signal and Noise Identification

Despite the advantages of using Gaussian signals pointed out in Section II, there are also several drawbacks associated with the separation between signal and noise components. In this case, the signal and noise share the same spectral positions obviating any straightforward separation in the frequency domain. Moreover, the signal component may be several orders of magnitude higher than the noise level.

A physical meaning solution, often used because of its practical interest, is to consider as signal the output component correlated with the input, as is usual in conventional rake receivers. This result is supported by Bussgang's theorem [9]. In Fig. 2, we can see a geometric illustration of this operation. The projection of the output (vector v)—which has correlated (collinear) components with the input and other ones uncorrelated (orthogonal)—onto the input signal component (vector u) is calculated using the input–output correlation and the power of input and output signals. That projection is the output signal component (vector w).

One way to obtain that correlated component is to use the BLA. The BLA is defined as the linear transfer function that is the best approximation to the nonlinear system in a least squares sense [6]. In the frequency domain, it can be given by

$$H_L(\omega) = \frac{S_{xy}(\omega)}{S_{xx}(\omega)} \tag{2}$$

where $S_{xy}(\omega)$ is the cross-spectral density of the input and output signals and $S_{xx}(\omega)$ is the input spectral density function that can be calculated as the Fourier transform of the cross-correlation and autocorrelation functions, respectively,

$$R_{xy}(\tau) = \overline{x(t)\,y(t+\tau)} = \int_{-\infty}^{\infty} x(t)\,y(t+\tau)\,dt \tag{3a}$$

$$R_{xx}(\tau) = \overline{x(t)\,x(t+\tau)} = \int_{-\infty}^{\infty} x(t)\,x(t+\tau)\,dt. \tag{3b}$$

Having defined this way the signal component, we can thus consider as nonlinear noise all the remaining output components. Part of this distortion noise is irrelevant as it falls out-of-band (i.e., around dc and the carrier harmonics) and, thus, can be eliminated by proper filtering. The remaining in-band noise is present in the co-channels and adjacent channels. To compute the SINAD, one must consider as relevant noise only the co-channel part.

The first approach considered is to calculate the output signal component in the case we have a memoryless nonlinearity modeled by a power series.

A. BLA Calculation for a Memoryless Nonlinearity

We will consider as input a Gaussian signal $x(t)$ so that the output is given by

$$y(t) = \sum_{n=1}^{N} \alpha_n x(t)^n. \tag{4}$$

In order to obtain the output signal component, we will evaluate the input–output cross-correlation. Applying the definition of (3) and the properties of averaging Gaussian random variables [5] $R_{xy}(\tau)$ will be

$$R_{xy}(\tau) = \alpha_1 R_{xx}(\tau) + 3\alpha_3 R_{xx}(0) R_{xx}(\tau) + 15\alpha_5 R_{xx}(0)^2 R_{xx}(\tau) + \cdots \tag{5}$$

which can be written in a generalized form as

$$R_{xy}(\tau) = R_{xx}(\tau) \cdot \sum_{n\text{odd}}^{N} \alpha_n \frac{(n+1)!}{\left(\frac{n+1}{2}\right)! 2^{\left(\frac{n+1}{2}\right)}} R_{xx}(0)^{\left(\frac{n-1}{2}\right)}. \tag{6}$$

In (6), we have a general result for input–output cross-correlation of a memoryless nonlinear system modeled by an Nth-order polynomial. This expression indicates that correlation only exists between output odd-order terms and the input since it is known that the average of the product of a number of Gaussian random variables is only nonzero if that number is even.

With (2) and (6), we can directly express the linear transfer function (or gain) of a memoryless nonlinearity modeled by a polynomial as

$$H_L(\omega) = \sum_{n\text{odd}}^{N} \alpha_n \frac{(n+1)!}{\left(\frac{n+1}{2}\right)! 2^{\left(\frac{n+1}{2}\right)}} R_{xx}(0)^{\left(\frac{n-1}{2}\right)}. \tag{7}$$

This expression states that the BLA is not only dependent on the system parameters α_i, but also on the input signal characteristics, namely, its even-order moments.

B. BLA Calculation for a Nonlinear System With Memory

Let us now address a nonlinear system that presents memory, but is sufficiently well behaved so that it can be described by a Volterra series. Although conceptually similar to the memoryless case, this problem is significantly more difficult to treat analytically. We will start the derivation process by writing the analytical expression for the output (8) as follows:

$$\begin{aligned} y(t) = &\int_{-\infty}^{+\infty} h_1(t-\sigma)\, x(\sigma)\, d\sigma \\ &+ \int_{-\infty}^{+\infty}\int_{-\infty}^{+\infty} h_2(t-\sigma_1, t-\sigma_2)\, x(\sigma_1)\, x(\sigma_2) d\sigma_1 d\sigma_2 \\ &+ \int_{-\infty}^{+\infty}\int_{-\infty}^{+\infty}\int_{-\infty}^{+\infty} h_3(t-\sigma_1, t-\sigma_2, t-\sigma_3) \\ &\cdot x(\sigma_1)\, x(\sigma_2)\, x(\sigma_3)\, d\sigma_1 d\sigma_2 d\sigma_3 + \cdots \end{aligned} \tag{8}$$

or, in a general form, as follows:

$$\begin{aligned} y(t) = \sum_{n=1}^{N} \int_{-\infty}^{+\infty} \cdots_{n\text{fold}} \int_{-\infty}^{+\infty} & h_n(t-\sigma_1, t-\sigma_2, \ldots, t-\sigma_n) \\ & \cdot x(\sigma_1) x(\sigma_2) \cdots x(\sigma_n) d\sigma_1 d\sigma_2 \cdots d\sigma_n. \end{aligned} \tag{9}$$

Once again, using the definition of cross-correlation (3), we will calculate the cross-correlation between input and output, considering a Gaussian random signal $x(t)$ and $y(t)$ given by (9), and $R_{xy}(\tau)$ in (10) as follows:

$$\begin{aligned} &R_{xy}(\tau) \\ &= \sum_n R_{xy_n}(\tau) \\ &= \int_{-\infty}^{+\infty} h_1(\tau-\sigma)\, R_{xx}(\sigma)\, d\sigma \\ &\quad + 3\int_{-\infty}^{\infty}\int_{-\infty}^{\infty}\int_{-\infty}^{\infty} R_{xx}(\tau-\sigma_1)\, R_{xx}(\sigma_2-\sigma_3) \\ &\quad \cdot h_3(\sigma_1, \sigma_2, \sigma_3)\, d\sigma_1 d\sigma_2 d\sigma_3 + \cdots \\ &= \sum_{n\text{odd}}^{N} \frac{(n+1)!}{\left(\frac{n+1}{2}\right)! 2^{\left(\frac{n+1}{2}\right)}} \int_{-\infty}^{+\infty} \cdots_{n\text{fold}} \int_{-\infty}^{+\infty} R_{xx}(\tau-\sigma_1) \cdots \\ &\quad \cdot R_{xx}(\sigma_{n-1}-\sigma_n)\, h_n(\sigma_1, \ldots, \sigma_n)\, d\sigma_1 \ldots d\sigma_n. \end{aligned} \tag{10}$$

Now we will use the same procedure of the last section to determine the BLA. We compute the Fourier transform of (10) and then use (2) to find $H_L(\omega)$. In order to find the Fourier transform of (10), we write $h_n(\tau_1, \ldots, \tau_n)$ as a function of the n-dimensional inverse Fourier transform of $H_n(\omega_1, \ldots, \omega_n)$. By changing the order of integration between ω's and σ's and using some simple properties of the Fourier transform, we will then reach (11) as follows:

$$\begin{aligned} &H_L(\omega) \\ &= \sum_{n\text{odd}}^{N} \frac{(n+1)!}{\left(\frac{n+1}{2}\right)! 2^{\left(\frac{n+1}{2}\right)}} \\ &\quad \cdot \int_{-\infty}^{+\infty} \cdots_{\frac{n-1}{2}\text{fold}} \int_{-\infty}^{+\infty} H_n\left(\omega, \omega_1, -\omega_1, \ldots, \omega_{\frac{n-1}{2}}, -\omega_{\frac{n-1}{2}}\right) \\ &\quad \cdot S_{xx}(\omega_1) \ldots S_{xx}\left(\omega_{\frac{n-1}{2}}\right) d\omega_1 \ldots d\omega_{\frac{n-1}{2}}. \end{aligned} \tag{11}$$

This expression (which to the best of the authors' knowledge is new) gives the BLA of a nonlinear dynamic system modeled by a Volterra series of order N when subject to a Gaussian input signal. It states that the BLA is dependent, not only on the system parameters and the even order moments of the input

(the integrated power), but also on the stimulus' power spectral density (PSD) [the shape of $S_{xx}(\omega)$]. The main interest of (11) resides in the fact that the BLA varies with the input signal PSD in a way that can be interpreted as if $S_{xx}(\omega)$ were "weighting" the nth-order Volterra kernel. Therefore, $H_L(\omega)$ will be different whenever $S_{xx}(\omega)$ gives more importance to the different parts of the multidimensional frequency response of each of the $H_n(\omega)$'s.

IV. Noise and Distortion Figure

Having developed the theoretical tools to isolate the signal components from the noise components, we are now able to define a new figure-of-merit that simultaneously deals with noise and distortion [10].

The relation between the NF and SNR, i.e., the ratio between signal and noise powers, is well known. As a matter of fact, although the NF is frequently referred to as the ratio between input and output SNRs, the IEEE-adopted formal definition of an NF is [11]

$$\mathrm{NF} = \frac{GN_o + N_a}{GN_o} \tag{12}$$

in which N_o is the output available noise power spectral densities at a given source noise temperature, as seen if the system were noise free, and N_a is the system's added noise, respectively. Defined this way, the NF varies with frequency and is, thus, also called the *spot NF*.

In a nonlinear system, the approach described above is incomplete [2] because the SNR degradation caused by the nonlinear intermodulation noise is not taken in account. Another common figure-of-merit, which is more useful in the context of nonlinear systems, is the SINAD. According to [12], it can be defined as the ratio of signal PSD to noise and distortion power spectral densities and can, thus, be expressed as

$$\mathrm{SINAD}_{\mathrm{lin}}(\omega) = \frac{S(\omega)}{N(\omega) + D(\omega)} \tag{13}$$

where $S(\omega)$, $N(\omega)$, and $D(\omega)$ are, respectively, the signal, additive noise, and nonlinear distortion power spectral densities.

It was already mentioned above that the NF can represent the ratio of SNR_i to SNR_o. If the same ratio is evaluated using the SINAD, a figure identical to the NF will be found, except that it will now also include the distortion impact. Accordingly, we will call it the NDF (14) as follows:

$$\begin{aligned}\mathrm{NDF}(\omega) &\equiv \frac{\mathrm{SINAD}_i(\omega)}{\mathrm{SINAD}_o(\omega)} \\ &= \frac{\dfrac{S_i(\omega)}{N_i(\omega)}}{\dfrac{|H_L(\omega)|^2 \cdot S_i(\omega)}{|H_L(\omega)|^2 \cdot N_i(\omega) + N_a(\omega) + \mathrm{IMD}(\omega)}} \\ &= \frac{|H_L(\omega)|^2 \cdot N_i(\omega) + N_a(\omega) + \mathrm{IMD}(\omega)}{|H_L(\omega)|^2 \cdot N_i(\omega)}.\end{aligned} \tag{14}$$

The NDF is thus defined as the ratio of the input SINAD to the output SINAD. In (14), $H_L(\omega)$ is the BLA, $N_i(\omega)$ is the input available noise PSD, $N_a(\omega)$ is the PSD of the additive noise introduced by the device, and $\mathrm{IMD}(\omega)$ is the PSD of intermodulation distortion (IMD) delivered to the load. For guaranteeing compatibility with the former IEEE NF definition, these

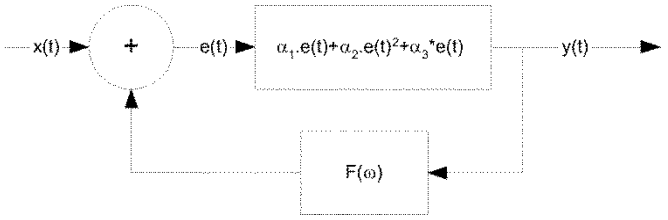

Fig. 3. Block diagram of a general nonlinear bandpass dynamic system.

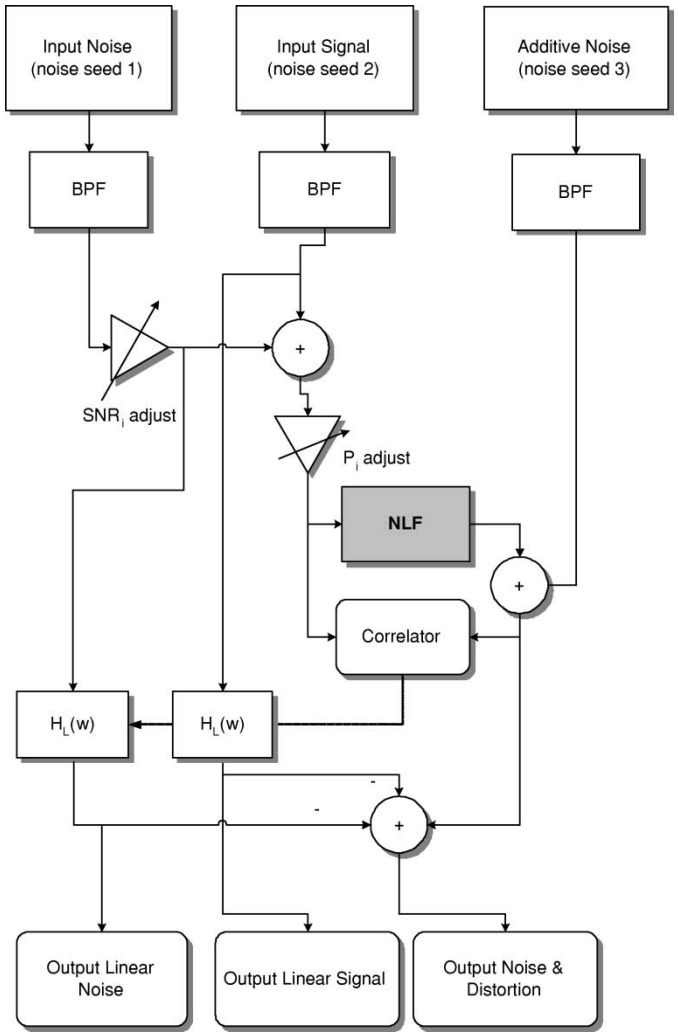

Fig. 4. Block diagram of the simulator used to validate NDF (NLF denotes nonlinear function).

SINADs describe spot frequency values and, thus, they are defined as the ratio between the spot signal PSD function to the sum of the spot PSD functions of the noise and distortion.

At the device's input port, these PSDs refer to the source available powers of the signal and noise when the source's equivalent noise internal resistance is at the standard noise temperature (290 K). The current NDF definition is, therefore, assuming that the signal available from the source is undistorted and, thus, that this situation must be guaranteed if the NDF is to be measured. In fact, what must be guaranteed is that the source's IMD cannot generate any appreciable IMD inside the device-under-test (DUT) and that its value, when seen at the DUT's output, is much smaller than the one due to the DUT itself.

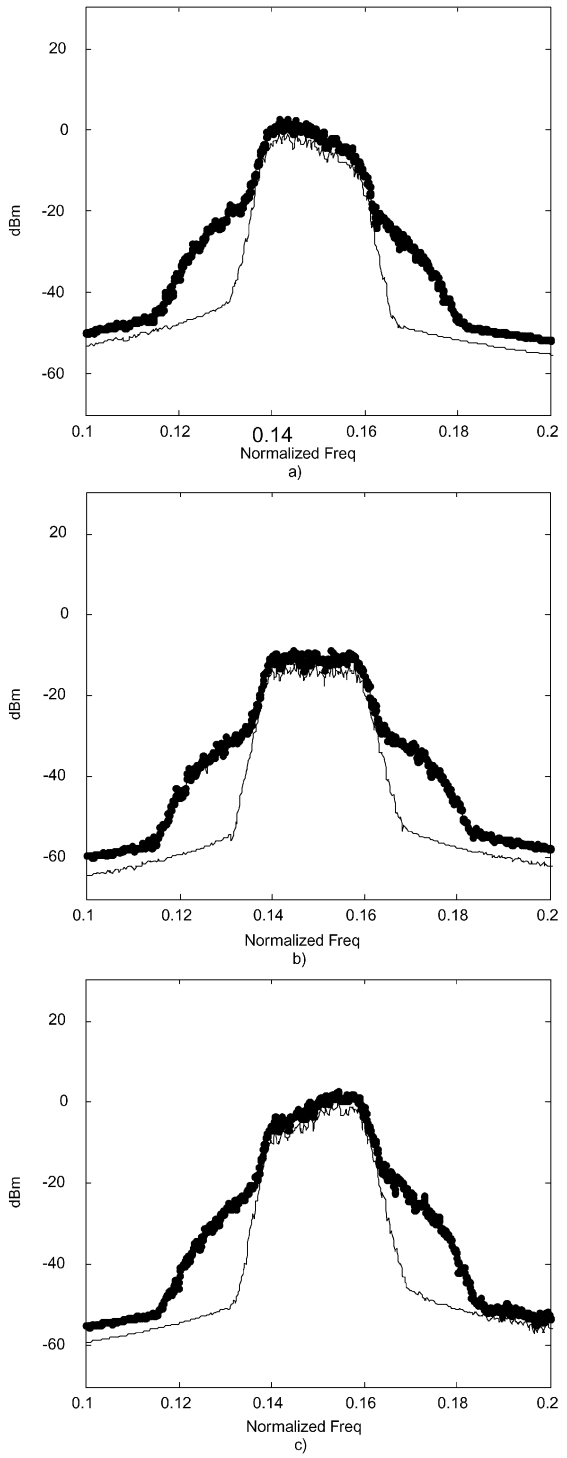

Fig. 5. Input spectrum of the test signals used for the BLA extraction (simple line) and output spectrum (dark line). (a) Signal spectrum 1. (b) Signal spectrum 2. (c) Signal spectrum 3.

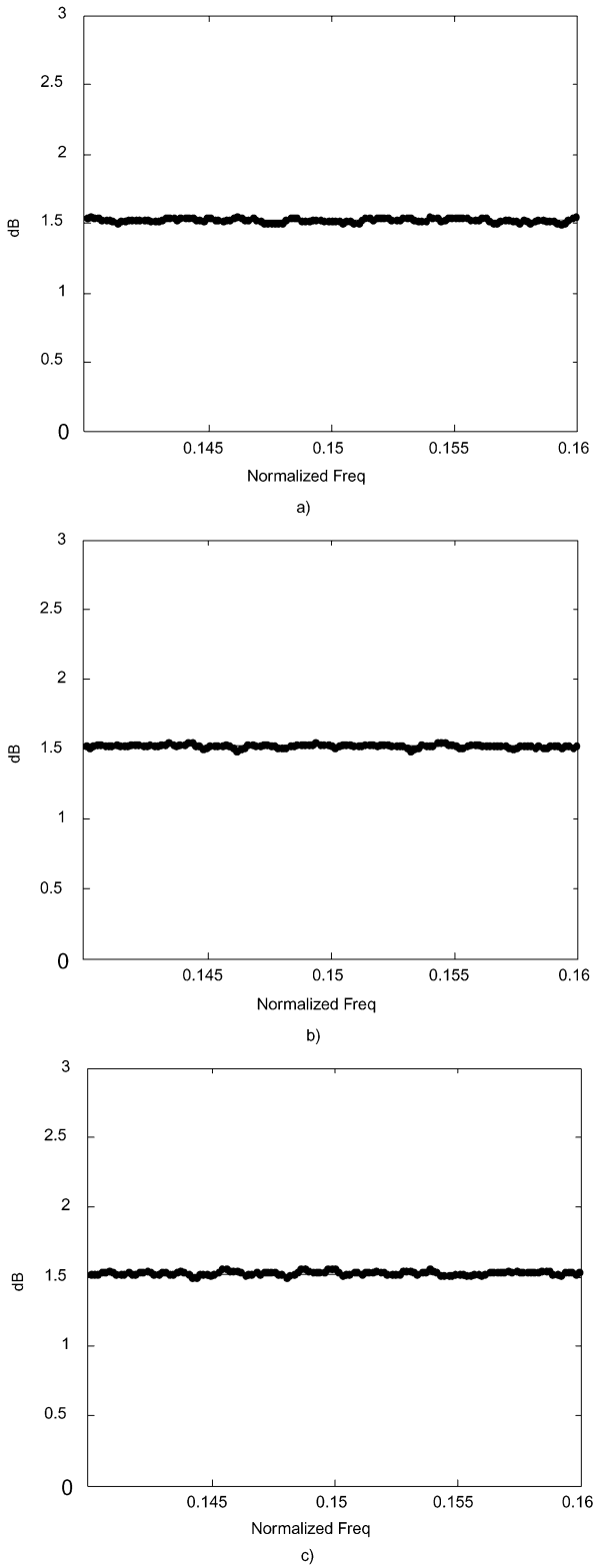

Fig. 6. In-band BLA: simulated (simple line); theoretical (dark line). (a) Signal spectrum 1. (b) Signal spectrum 2. (c) Signal spectrum 3.

When SINAD calculations are to be made with this NDF, and the device is isolated, it is naturally expected that the input IMD is zero since the source can be supposed to produce an undistorted signal. However, if that is not the case, or if the device is embedded in a chain whose precedent blocks already generate some distortion, then this available distortion PSD should be added to the source available PSD of the signal and the additive noise (since all three are assumed uncorrelated).

Note, however, that, in this latter case, a precise calculation of the total output IMD would require knowledge of the phase of those distortion components since, being correlated with the ones generated by the DUT, they cannot be simply added in power at the output. However, the more usual practical situation is that the precise IMD phase relations are unknown, and

no other alternative is then left to rely on a mere absolute value addition. Such a power wise addition would, therefore, correspond to an average power value, as discussed in [13].

At the output port, the situation is a little bit more complex, as the DUT's IMD depends on the load termination. Thus, we will have to consider the actual load impedance and define the output PSDs of the signal, IMD, and noise as referring to the actual powers delivered to that load. That is, while the IEEE NF definition assumes that the DUT is a system that can be described by an operator whose input variables are the available source PSDs, and the output variables are the available output PSDs, we now have to assume that our system is represented by an operator whose input variables are the input available PSDs, while the output variables are the PSDs delivered to the load.

In practice, however, these two distinct definitions will lead to similar values in the vast majority of situations. Indeed, since the output mismatch suffered by the signal is the same as the one suffered by the noise, the ratio of their PSDs (the SNR, which is essential in NF calculation) is an invariant to load impedance. Thus, an NF defined from output available PSDs, or another one defined from PSDs actually delivered to the load, will only differ if the noise introduced by the load (thermal noise) is significant compared to the noise delivered to that load by the DUT, and since the equivalent noise temperature of the load and the source are probably the same, this can only happen if a rare situation of a DUT with small gain and very low added noise is to be characterized. Therefore, significant discrepancies between our NDF and the previous IEEE NF will only be noticed for DUTs of very small gain and very low added powers of additive noise and distortion. If the load added noise PSD were subtracted from the total noise PSD measured at the load (indeed, it can be subtracted because the noise associated to the load is uncorrelated to any other noise generated in the measurement system), then the NDF and the IEEE NF would again be perfectly consistent.

Finally, since the IEEE NF was originally defined for linear systems, it was always a measure of the system's induced SNR degradation independent of the signal input power. That is so because, keeping the gain constant, the output SNR becomes independent of the input signal power or noise power. On the contrary, the NDF is especially useful for nonlinear systems where the gain and generated IMD are strongly dependent on the input power. Therefore, it should be of no surprise that the NDF must be defined for a certain input power. In the case of dynamic nonlinear systems, the BLA of (11) actually shows that it will even be dependent on the available signal's PSD.

To exemplify the use of the NDF, a nonlinear system excited by an input $x(t)$ composed of a signal $s(t)$ and noise $n(t)$ is considered $[x(t) = s(t) + n(t)]$. The SINAD_o can be calculated if the output signal, noise, and distortion components are separately identified. As stated above, those components can be separated using the BLA. With input $x(t)$, the output $z(t)$ can be decomposed in

$$z(t) = h_L(t) * x(t) + y(t) \tag{15}$$

where $y(t)$ is uncorrelated with $x(t)$ and has two distinct components: the additive noise introduced by the system and the generated nonlinear distortion. Since the origin of these two components is physically distinct, they are uncorrelated with each other and can thus be added in power. The value of $h_L(t)$ can be determined using the BLA. According to this formulation, the following output signal component was found: $h_L(t) * x(t)$, i.e., the output signal is the output component that can be obtained with the linear transfer function derived from the input output cross-correlation. With all these statements, we can write the SINAD_o as

$$\mathrm{SINAD}_o(\omega) = \frac{|H_L(\omega)|^2 \cdot S_i(\omega)}{|H_L(\omega)|^2 \cdot N_i(\omega) + N_a(\omega) + \mathrm{IMD}(\omega)}. \tag{16}$$

In this expression, $S_i(\omega)$ and $N_i(\omega)$ denote the input signal and input noise power spectral densities, respectively. $H_L(\omega)$ is the BLA transfer function, $N_a(\omega)$ is the PSD of the DUT's induced additive noise, and $\mathrm{IMD}(\omega)$ is the PSD of the stochastic nonlinear IMD.

The NDF will now be computed for a particular case of the input and for a nonlinear memoryless system where the signals are flat over a bandwidth B with power P_s and P_n, given by (17) as follows:

$$S_{ss}(\omega) = \begin{cases} \dfrac{P_s}{2B}, & -\omega_H \le \omega \le -\omega_L; \quad \omega_L \le \omega \le \omega_H \\ 0, & \text{elsewhere} \end{cases}$$
$$S_{nn}(\omega) = \begin{cases} \dfrac{P_n}{2B}, & -\omega_H \le \omega \le -\omega_L; \quad \omega_L \le \omega \le \omega_H \\ 0, & \text{elsewhere.} \end{cases} \tag{17}$$

The output PSD in the fundamental zone may be obtained, replacing (17) in (4), up to the third order, and can be written as

$$\begin{aligned} S_{yy}(\omega) = {} & \left[\alpha_1^2 + 6\alpha_1\alpha_3(P_s + P_n) + 9\alpha_3^2(P_s + P_n)^2\right] \\ & \cdot \frac{(P_s + P_n)}{2B} \\ & + 6\alpha_3^2\left(-\omega^2 + (\omega_L + \omega_H)\omega + \frac{B^2}{2} - \omega_L\omega_H\right) \\ & \cdot \frac{3}{8B^3}\left(P_s^3 + P_n^3 + 3P_s^2P_n + 3P_sP_n^2\right). \end{aligned} \tag{18}$$

Using (7), we can identify the signal components in (18) and isolate them from nonlinear distortion. Also taking into account the effect of additive noise, the in-band output SINAD can be obtained, as depicted in (19), shown at the bottom of this page.

$$\mathrm{SINAD}_o(\omega) = \frac{\left[\alpha_1 + 3\alpha_3(P_s + P_n)\right]^2 \frac{P_s}{2B}}{\left[\alpha_1 + 3\alpha_3(P_s + P_n)\right]^2 \frac{P_n}{2B} + 6\alpha_3^2\left(-\omega^2 + (\omega_L + \omega_H)\omega + \frac{B^2}{2} - \omega_L\omega_H\right) \cdot \frac{3 \cdot (P_s + P_n)^3}{8B^3} + N_a} \tag{19}$$

Using (14) and (19), in-band $\mathrm{NDF}(\omega)$ for this case is given by (20), shown at the bottom of this page, where we can see that the NDF assumes a parabolic pattern inside the band. That is due to the triple convolution of the bandpass signal used in this example.

This expression will not tend to (1) since the statistical properties of Gaussian noise (even when the bandwidth is narrow) are different from a single sinusoid.

In the case of a nonlinear system with memory, the process is much more laborious, but follows exactly the same procedure. We first calculate the BLA using (11), then derive the output spectral density, and use these two values to compute output noise and distortion.

V. Validation of the Theoretical Results

In order to validate the above theory, the NDF of the general system of Fig. 3 was estimated from time-domain numerical simulations, and these results were compared to the ones directly obtained from (14). Several tests were performed for different input signals and distinct system configurations.

The Volterra series representation of the system in Fig. 3 was obtained in [14] and is rewritten here for convenience as follows:

$$H_1(\omega) = \frac{\alpha_1}{D(\omega)} \tag{21}$$

and

$$\begin{aligned} &H_3(\omega_1,\omega_2,\omega_3) \\ &= \frac{1}{D(\omega_1)D(\omega_2)D(\omega_3)}\frac{1}{D(\omega_1+\omega_2+\omega_3)} \\ &\cdot\left\{\alpha_3+\frac{2}{3}{\alpha_2}^2\left[\frac{F(\omega_1+\omega_2)}{D(\omega_1+\omega_2)}+\frac{F(\omega_1+\omega_3)}{D(\omega_1+\omega_3)}+\frac{F(\omega_2+\omega_3)}{D(\omega_2+\omega_3)}\right]\right\} \end{aligned} \tag{22}$$

where $D(\omega) = 1 - \alpha_1 F(\omega)$.

This general system can be set to model both situations presented above, i.e., the memoryless nonlinear system and the system with memory.

The memoryless nonlinear system is obtained by eliminating the feedback path, making $F(\omega) = 0$, while the system with memory is obtained by proper tuning of the feedback path. In [14], it was proven that only an $F(\omega)$ reactive to the base band frequencies can be responsible for the envelope memory effects. Thus, in the dynamic case, $F(\omega)$ was designed in order to present some reactive behavior at low frequencies.

In order to observe the impact of the input signal spectrum on the BLA and, thus, on the NDF, in the dynamic case, we will simulate this system recurring to three different input signals.

The simulator block diagram is depicted in Fig. 4.

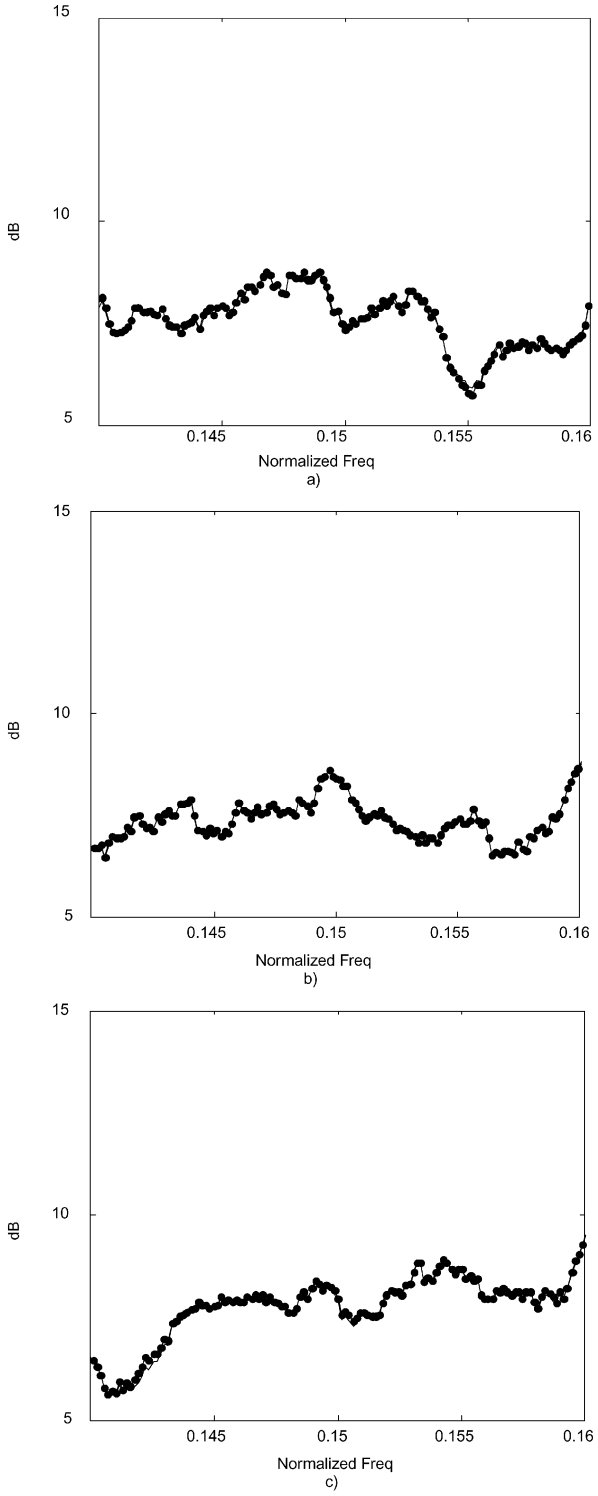

Fig. 7. In-band NDF: simulated (simple line), theoretical (dark line). (a) Signal spectrum 1. (b) Signal spectrum 2. (c) Signal spectrum 3.

$$\mathrm{NDF}(\omega) = \frac{\left[\alpha_1 + 3\alpha_3(P_s+P_n)\right]^2 P_n + \frac{9}{2}\alpha_3^2\left(-\omega^2 + (\omega_L+\omega_H)\omega + \frac{B^2}{2} - \omega_L\omega_H\right)\frac{(P_s+P_n)^3}{B^2} + N_a}{\left[\alpha_1 + 3\alpha_3(P_s+P_n)\right]^2 P_n} \tag{20}$$

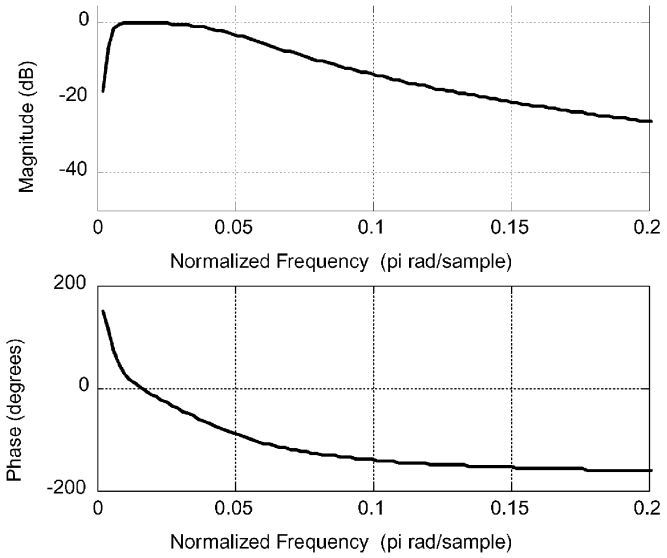

Fig. 8. Frequency response of the feedback filter $F(\omega)$ used.

A. NDF Calculation in a Memoryless Situation

Lets consider first a memoryless nonlinearity $(F(\omega) = 0)$. Although the theoretical conclusions stated that the BLA is constant with the input spectrum in memoryless nonlinear systems, three different spectrums are used in order to compare it with the behavior of systems including memory.

Fig. 5 depicts the input spectrum of each test signal used. In this figure, the output spectrum is also plotted, where the adjacent-channel distortion generated in the nonlinearity can be observed.

As can be seen in Fig. 6, the BLA is unaffected by the input signal spectrum shape. This confirms the theoretical results previously obtained in Section III, which state that the $H_L(\omega)$ of (7) is only dependent on the even-order moments of the input signal and not on its shape.

Although the BLA is an invariant to the input spectrum shape, the NDF varies with it. This variation is due to the fact that, in the frequency zones where the input signal spectral density is higher, the nonlinear distortion level increases at a faster rate than the output signal. Hence, the NDF must also present higher values. Furthermore, if the input spectral density has a flat shape (signal spectrum 2), the output nonlinear distortion has parabolic shape, as predicted in (20). That is mildly seen on Fig. 7(b).

B. NDF Calculation in a Nonlinear System With Memory

In order to calculate the BLA for a nonlinear system with memory, a polynomial with α_1 and α_3 identical to the memoryless case was used, but α_2 was increased to give more emphasis to the memory effect that we are looking for [14], [15]. Note that, in (22), despite the increase of the polynomial second degree coefficient α_2, we are also varying the third-order Volterra kernel [14]. A low-frequency feedback filter $F(\omega)$ with frequency response, shown in Fig. 8, was introduced.

Note that this filter has a rejection ratio of over 20 dB in the fundamental frequency zone and a steep rolloff at the low frequencies from 0 to $Bw/2$ (Bw of the signals used were approximately 2% of the sampling frequency).

Fig. 9 shows the input and output spectra of the test signals used. The output has an adjacent distortion level higher than the one used when compared to the memoryless case (Fig. 5). This is a consequence of the fact that, in this case, the strong second-order coefficient also contributes to in-band distortion due to the feedback path, as seen in (22).

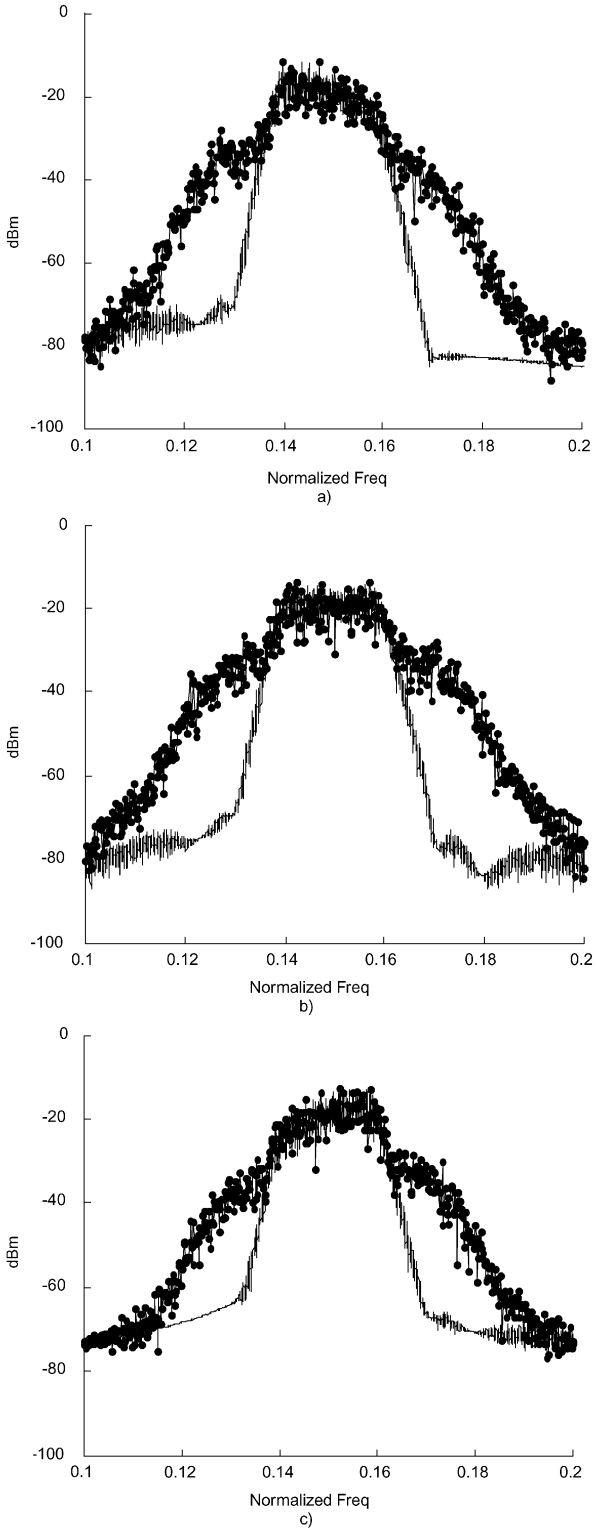

Fig. 9. Input spectrum of the test signals used for the BLA extraction (simple line) and output spectrum (dotted line). (a) Signal spectrum 1. (b) Signal spectrum 2. (c) Signal spectrum 3.

The valley shown in the BLA plot of Fig. 10(b) is due to the high-pass characteristic of the feedback filter manifested be-

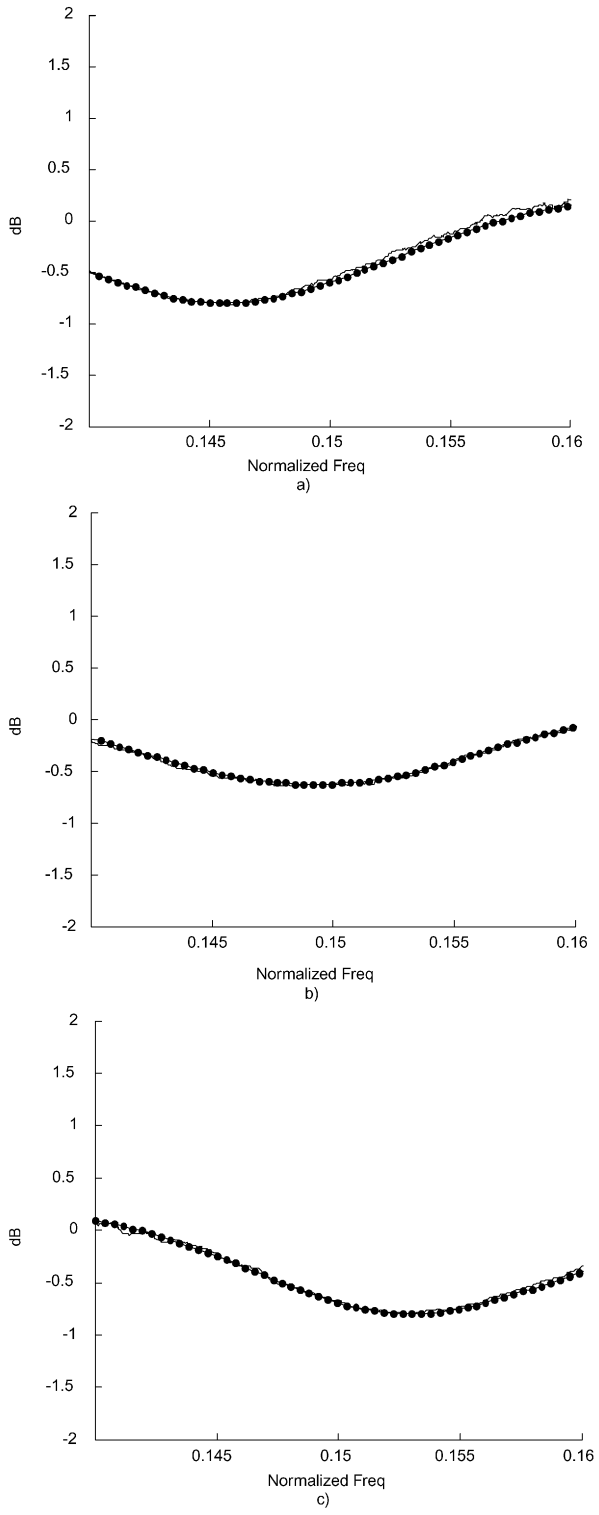

Fig. 10. In-band BLA: simulated (simple line); theoretical (dotted line). (a) Signal spectrum 1. (b) Signal spectrum 2. (c) Signal spectrum 3.

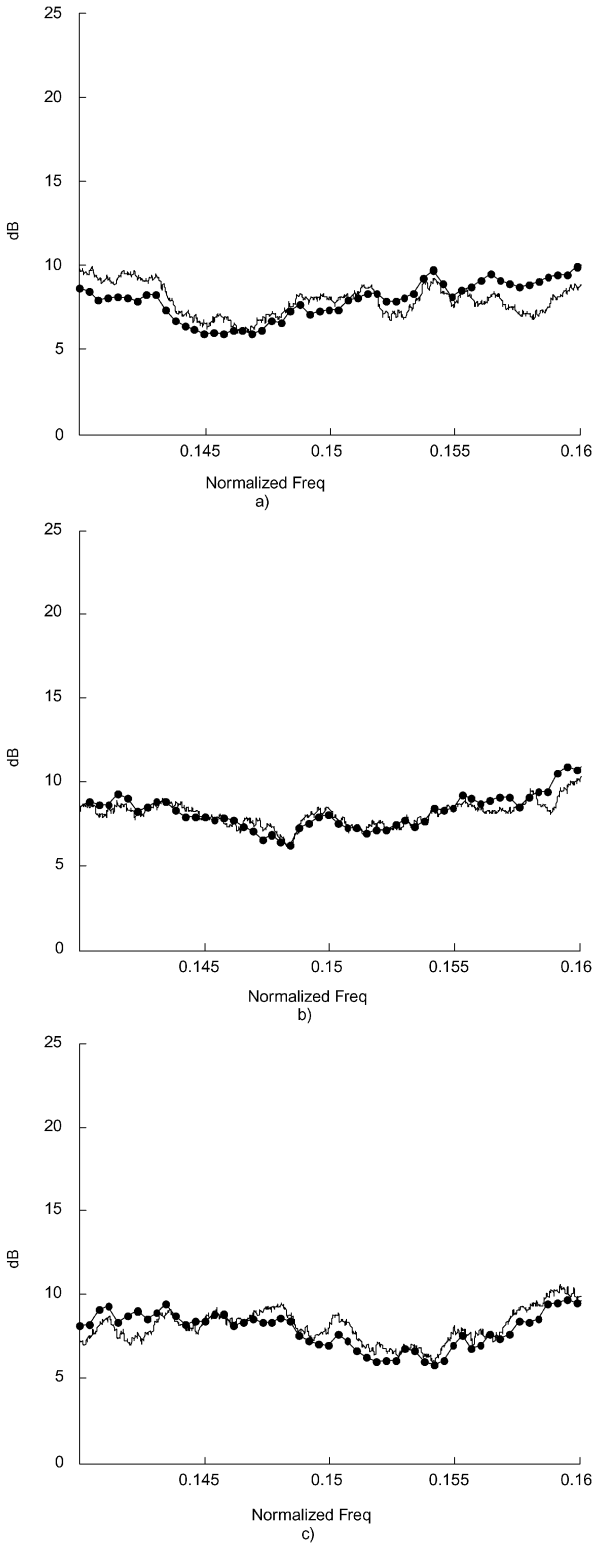

Fig. 11. In-band NDF: simulated (simple line); theoretical (dotted line). (a) Signal spectrum 1. (b) Signal spectrum 2. (c) Signal spectrum 3.

tween dc and 0.02, as $F(\omega)$ increases from the center of the band (dc) to the extremes ($\pm Bw$, the occupied signal bandwidth). This effect can only be noticed in this figure because that case is the only resulting from a flat input spectrum. For the input spectra 1 and 3 [see Fig. 10(a) and (c)], and due to the dynamic behavior of the feedback path, the BLA is affected simultaneously by the input spectrum and filter shapes, this way reducing the effect of the filter form.

The residual differences seen between theoretical and simulated results are due to the fact that the noise signal in use here is not of infinite length, but a limited sequence whose realizations were averaged in frequency.

In Fig. 11, the NDF is also presented and, as theoretically predicted, also varies with the input spectrum.

VI. Conclusions

In this paper, the misleading result presented in [2] was discussed, and its main drawbacks pointed out. Nevertheless, the important conclusion obtained in [2], stating that the usual NF standard is affected by nonlinearities, is used to propose a new figure-of-merit, called the NDF, which relates the input and output SINADs. Therefore, an NDF definition for nonlinear systems, but still consistent with the traditional linear NF, was advanced.

Additionally, and in order to analytically characterize the NDF, the BLA was calculated for memoryless and dynamic systems. In the memoryless case, it was shown that BLA is only dependent on the nonlinearity and input power. In dynamic systems, however, it also changes with the input spectrum shape.

The excellent agreement between simulated and theoretical results gives us confidence to use this figure-of-merit in link budget designs.

References

[1] D. M. Pozar, *Microwave and RF Wireless Systems*. New York: Wiley, 2001.

[2] A. Geens and Y. Rolain, "Noise figure measurements on nonlinear devices," *IEEE Trans. Instrum. Meas.*, vol. 50, pp. 971–975, Aug. 2001.

[3] H. Ku, M. D. Mc Kinley, and J. S. Kenney, "Quantifying memory effects in RF power amplifiers," *IEEE Trans. Microwave Theory Tech.*, vol. 50, pp. 2843–2849, Dec. 2002.

[4] J. H. K. Vuolevi, T. Rahkonen, and J. P. A. Manninen, "Measurement technique for characterizing memory effects in RF power amplifiers," *IEEE Trans. Microwave Theory Tech.*, vol. 49, pp. 1383–1389, Aug. 2001.

[5] M. Schetzen, *The Volterra and Wiener Theories of Nonlinear Systems*. New York: Wiley, 1980.

[6] R. Pintelon and J. Schoukens, *System Identification—A Frequency Domain Approach*. Piscataway, NJ: IEEE Press, 2001.

[7] N. Blachman, "Bandpass nonlinearities," *IEEE Trans. Inform. Theory*, vol. IT-10, pp. 162–164, Apr. 1964.

[8] ——, "The effect of a large signal upon a small signal in a memoryless nonlinear bandpass amplifier," *IEEE Trans. Commun.*, vol. COM-29, pp. 72–73, Jan. 1981.

[9] H. E. Rowe, "Memoryless nonlinearities with Gaussian inputs: Elementary results," *Bell Syst. Tech. J.*, vol. 71, no. 7, pp. 1519–1525, Sept. 1982.

[10] P. M. Lavrador, N. B. Carvalho, and J. C. Pedro, "Noise and distortion figure—An extension of noise figure definition for nonlinear devices," in *IEEE MTT-S Int. Microwave Symp. Dig.*, Philadelphia, PA, 2003, pp. 2137–2140.

[11] *IEEE Standard Dictionary of Electrical and Electronics Terms*, 4th ed. New York: IEEE, 1988.

[12] T. C. Hofner, "Defining and testing dynamic ADC parameters," *Microwaves RF*, pp. 75–84 and 162, Nov. 2000.

[13] J. C. Pedro and N. B. Carvalho, *Intermodulation Distortion in Microwave and Wireless Circuits*. Norwood, MA: Artech House, 2003.

[14] J. C. Pedro, N. B. Carvalho, and P. M. Lavrador, "Modeling nonlinear behavior of band-pass memoryless and dynamic systems," in *IEEE MTT-S Int. Microwave Symp. Dig.*, Philadelphia, PA, 2003, pp. 2133–2136.

[15] N. B. de Carvalho and J. C. Pedro, "A comprehensive explanation of distortion sideband asymmetries," *IEEE Trans. Microwave Theory Tech.*, vol. 50, pp. 2090–2101, Sept. 2002.

Pedro Miguel Lavrador (S'02) was born in Mira, Portugal, in 1978. He received the Diploma degree in electronics and telecommunications engineering from the University of Aveiro, Aveiro, Portugal, in 2001, and is currently working toward the Ph.D. degree in nonlinear systems at the University of Aveiro.

Since October 2000, he has been with the Telecommunications Institute, University of Aveiro. His main research interests are the study of the impact of nonlinear effects in communication systems, and efficient simulation methods and models for the same types of systems.

Mr. Lavrador was the three-time recipient of the prize for students with the best grades of engineering courses at the University of Aveiro.

Nuno Borges de Carvalho (S'92–M'00) was born in Luanda, Portugal, in 1972. He received the Diploma and Doctoral degrees in electronics and telecommunications engineering from the University of Aveiro, Aveiro, Portugal, in 1995 and 2000, respectively.

From 1997 to 2000, he was an Assistant Lecturer with the University of Aveiro, where he currently is an Auxiliary Professor and a Senior Research Scientist with the Telecommunications Institute. He has been engaged with different projects on nonlinear computer-aided design (CAD) and circuits. He coauthored *Intermodulation in Microwave and Wireless Circuits* (Norwood, MA: Artech House, 2003). His main research interests include CAD for nonlinear circuits and design of RF microwave power amplifiers. He has been a reviewer for several magazines.

Dr. Carvalho is a member of the Portuguese Engineering Association. He is a member of the Editorial Board for the IEEE Transactions on Microwave Theory and Techniques. He was the recipient of the 1995 University of Aveiro and the Portuguese Engineering Association Prize for the best student at the University of Aveiro, the 1998 Student Paper Competition (third place) presented at the IEEE International Microwave Symposium, and the 2000 Institution of Electrical Engineers, U.K., Measurement Prize.

José Carlos Pedro (S'90–M'95–SM'99) was born in Espinho, Portugal, in 1962. He received the Diploma and Doctoral degrees in electronics and telecommunications engineering from the University of Aveiro, Aveiro, Portugal, in 1985 and 1993, respectively.

From 1985 to 1993, he was an Assistant Lecturer at the University of Aveiro, where, in 1993, he became an Assistant Professor. He is currently an Associate Professor and a Senior Research Scientist in the Telecommunications Institute at the university. His main scientific interests include active device modeling and the analysis and design of various nonlinear microwave and optoelectronics circuits, in particular, the design of highly linear multicarrier power amplifiers and mixers. He has authored or coauthored several papers published in international journals and presented at symposia. He coauthored *Intermodulation Distortion in Microwave and Wireless Circuits* (Norwood, MA: Artech House, 2003).

Dr. Pedro has served as a reviewer for the IEEE Transactions on Microwave Theory and Techniques and the IEEE Microwave Theory and Techniques Society (IEEE MTT-S) International Microwave Symposium (IMS). He was the recipient of the 1993 Marconi Young Scientist Award and the 2000 Institution of Electrical Engineers (IEE), U.K., Measurement Prize.